

# GPS COMPOSITE CLOCK SOFTWARE PERFORMANCE

A. L. Satin, W. A. Feess, H. F. Fliegel, and C. H. Yinger  
The Aerospace Corporation  
Los Angeles, CA 90009

## ABSTRACT

*Computer software for ensembling all the space vehicle (SV) and ground clocks of the Global Positioning Systems (GPS) was implemented at the Master Control Station (MCS) on 17 June 1990. Improved GPS time stability and steering control are predicted. This paper assesses the perceptions of both Air Force and outside users and compares current performance to theoretical predictions.*

## GPS SYSTEM DESCRIPTION

The Global Positioning System is a Department of Defense space-based navigation and timing dissemination system currently under deployment. By 1993 it will consist of a constellation of 24 space vehicles (SVs) supported by a control segment (CS) that tracks the SVs with its monitor stations (MSs), determines SV ephemeris states and SV and MS clock states at the Master Control Station (MCS) and periodically uploads the SVs with predicted SV states that users require to navigate and/or determine their time. At this stage in the buildup, the constellation consists of six block I SVs and nine block II SVs. The CS MSs are located at Kwajalein Island, Diego Garcia Island, Hawaii, Ascension Island, and Colorado Springs, Colorado.

SV range measurements (i.e., pseudorange) are a function of the SV(i)-MS(j) geometric range and the phase offset between the SV(i) and MS(j) clocks, where i and j are the ith SV and the jth MS, respectively. The accuracy with which a user can navigate (i.e., determine his position and clock state) depends on the accuracy of his measured pseudorange and the accuracy of the predicted SV ephemeris and clock information, generated and uploaded by the CS. The latter source of error is fundamental to GPS operation and is quantified by the User Range Error (URE). URE is defined as the difference between the range-to-a-user computed using predicted states and the "true" range-to-a-user computed using the latest Kalman estimates of ephemeris and clock. Operationally, the MCS computes UREs every 15 min (the Kalman filter update cycle) for each SV, taking a root sum of squares (RMS) of individual UREs to a fixed set of grid locations on the earth that have visibility to the SV.

The CS, by solving for SV and MS clock phase and frequency states from the pseudorange measurements, effectively synchronizes the system to GPS time. Originally the GPS time reference was taken to be one of the MS clocks. States for that MS (i.e., the master MS) were defined to be fixed at zero and, hence, were not included in the filter state vector. Clock state offsets estimated by the filter were then relative to master clock (GPS) time. When the filter is allowed to estimate all clock states (i.e., including states for what used to be the master MS), the configuration is called a composite or ensemble clock system. Since June of this year, the time reference for the system clocks (i.e., GPS time) has been a composite clock.

Since the MCS has so many SV states to estimate (11 per SV  $\times$  24) it was decided long ago to "partition" the SVs among several filters each capable of handling up to six of them and each containing, of course, the complete complement of MS states: 3 per MS  $\times$  4 for a master clock configuration and 3 per MS  $\times$  5 for the composite clock case.

## COMPOSITE CLOCK IMPLEMENTATION AND THEORY

When additional states are added to the Kalman filter, for what was the master MS, the GPS system becomes explicitly unobservable. This is because a constant bias shift in all clock phase states would not affect pseudorange and hence, would be unobservable to the filter. The existence of this unobservable component of state causes the clock phase covariance matrix to grow linearly with time even though the system is completely stable with well behaved filter gains. See Reference 1 for further discussion of these characteristics. Since a growing covariance matrix will eventually cause numerical problems, a method for reducing the covariance matrix without degrading filter performance was introduced. The method chosen was reduction via pseudomeasurement update (Reference 2).

### Covariance Reduction

This update takes the standard Kalman form

$$P' = P - [PH^T(HPH^T + R)^{-1}] HP \quad (1)$$

where  $P'$  is the covariance matrix resulting from the update (i.e., the reduced covariance matrix) and  $R$  is the pseudomeasurement noise variance. The matrix  $P$  in Equation 1 is the full  $n \times n$  covariance matrix of ephemeris and clock states for the SVs and MSs of a particular partition. All filter partitions undergo independent covariance reductions every filter update cycle. The  $n \times 1$  column vector  $H^T$  is constructed by inserting each element of an  $m \times 1$  column vector  $\hat{H}^T$  into the appropriate position in an  $n \times 1$  vector of zeros.  $\hat{H}^T$  is given by

$$\hat{H}^T = B^{-1}u/[u^T B^{-1}u] \quad (2)$$

where  $B$  is the  $m \times m$  submatrix of  $P$  corresponding to clock phase states only and  $u$  is an  $m \times 1$  column vector of elements, all of which are one. Each clock in a partition, then, has an ensembling weight in the column vector  $H$  (ordered as  $P$  is ordered), whereas each ephemeris state has weight zero. By the construction of  $H$ , the sum of all weights is one. Equation 2 assigns to each clock a normalized set of phase and frequency weights that are inversely proportional to the magnitude of estimation error variance (i.e., the diagonals of  $B$ ). Because of the particular form of  $H^T$ , however, the correction term in Equation 1, i.e., the second term on the right side of the equation has nonzero elements corresponding to ephemeris states and, hence, this method of covariance reduction is not a transparent variation on filter operation. A simulation of this algorithm was performed (Reference 3) using real pseudorange measurement data from the MCS in order to assess the impact of the algorithm on Kalman states and URE. RMS UREs were shown to be very good with the algorithm and states changed only slightly. Ephemeris states with composite clock operation are unchanged from

what they were with the master clock configuration—with or without the reduction algorithm (Reference 3).

#### Partition Reconciliation

Partition reconciliation is required to ensure that composite clock time for the various filter partitions is consistent. Uploads built for SVs from different partitions must have very nearly the same reference time for clock phase and frequency offsets contained in the navigation message. Any difference in reference times maps into URE. The reconciliation process, since it is an adjustment of reference time for the partition, does not affect filter gains or measurement residuals because it amounts to a constant shift of all the clock phase and frequency states in the partition. Each partition will have a different shift as computed by the reconciliation algorithm. Partition reconciliation is possible only because the MS clocks are common to each partition. It requires that a specified weighted sum of MS states be the same for each partition, where the same weights are used to compute the sum for each partition. The value of the weighted sum is itself a weighted average of MS and SV states. The computation proceeds as follows:

First the vectors  $\bar{b}_i$  are computed for each partition according to (References 2, 4)

$$\bar{b}_i = [(H^*)^T C^{-1} H^*]^{-1} (H^*)^T C^{-1} \begin{bmatrix} \hat{\phi}_i^1 \\ \vdots \\ \hat{\phi}_i^5 \end{bmatrix} \quad (3)$$

where  $\hat{\phi}_i^j$  are the MS<sub>j</sub> clock states for the i<sup>th</sup> partition and  $H^*$  is a  $10 \times 2$  matrix of five  $2 \times 2$  identity matrices.  $C$  is a  $10 \times 10$  matrix obtained by summing the MS clock covariance submatrices from the various partitions. Note from Equation 3 that the linear combination of MS states is taken for each partition. Next, the vector  $\bar{b}$  that the  $\bar{b}_i$  are reconciled to, is computed according to Equation 4 below:

$$\bar{b} = W^{-1} \sum_{i=1}^N w_i \bar{b}_i \quad (4)$$

where

$$w_i = \sum_{j=1}^{n_i} [p_i^j]^{-1}, \quad W = \sum_{i=1}^N w_i$$

$N$  = the number of partitions, and  $n_i$  = the number of SVs in partition i.

$$p_i^j = \begin{bmatrix} q_1^j \tau + q_2^j \tau^3 / 3 & q_2^j \tau^2 / 2 \\ q_2^j \tau^2 / 2 & q_2^j \tau \end{bmatrix} \quad (5)$$

for the j<sup>th</sup> SV in partition i. In Equation 5,  $q_1^j$  and  $q_2^j$  are the phase and frequency process noise covariances, respectively, and  $\tau$  is the update interval (15 min). The adjustment ( $\Delta b_i$ ) that gets applied to each clock phase state in partition i is then computed by

$$\Delta b_i = \bar{b} - \bar{b}_i$$

After the adjustments are made to each partition, a recomputation of the  $\tilde{b}_i$  would yield  $\bar{b}$  for all partitions. This means that GPS time for each partition is now the same, i.e., after reconciliation the weighted average of MS states for each partition is the same.

#### Stability of GPS Time

One of the primary reasons for ensembling the GPS clocks (i.e., constructing a composite clock) is to gain stability in GPS time. Clock ensembling is a proven technology most prominently used by the U.S. Naval Observatory (USNO) and National Institute of Standards and Technology (NIST). The enhancement of stability for a system of  $n$  clocks, each of which is stable to say 1E-13, goes as  $1/\sqrt{n}$ . For the current system of 19 clocks, operating with a Kalman filter configured for the composite clock option, the stability of GPS time is predicted to be of the order of 2.3E-14. This assumes that the three MCS filter partitions (with 5, 5 and 4 SVs in partitions 1, 2, and 3, respectively) are being reconciled perfectly and states do not differ appreciably from what they would be if the MCS were operating with the 14 SVs in one partition.

#### Steering of GPS Time

The composite clock software package provides a new GPS time steering algorithm that automatically determines and applies the appropriate clock drift rate steer to all clock states when enabled by operator directive. The operator need only input daily USNO updates of GPS-UTC phase offset. A bang-bang controller (Reference 4) has been implemented. Allowable steering rates are  $\pm 2\text{E-}19\text{s/s}^2$  and 0. Three steering modes are provided as follows: steer out the GPS-UTC offset as computed by the MCS from "raw" USNO measurements; steer out a particular GPS-UTC offset input by the operator; or steer GPS time to one of the MS clocks. Simulations of this control loop, carried out by The Aerospace Corporation (Reference 5), predict an RMS steady state control error of the order of 10 ns assuming the GPS time stability is 3E-14s/s at 1 day (Figure 1).

### COMPOSITE CLOCK PERFORMANCE (ACTUAL)

Transition to the composite clock was initiated on 17 June 1990 by including the master MS clock states as estimated states in the filter partitions. This act causes the state component covariances to then be Q'd (i.e., process noise added in the filter propagation operation) every 15 min.

#### UREs

RMS UREs for all age-of-data were as good, if not better, than what they were with the master clock configuration. For one upload per day per SV these RMS values were in the range of 2 to 4 m. Note that UREs are very insensitive to GPS time stability. They are primarily due to SV clock phase/frequency variations over the upload interval.

### Steering of GPS Time

At 23:30 on 25 June 1990 (MJD48067), a directive was input to the system to begin steering GPS time to drive the GPS-UTC internally computed offset to zero. Figure 2 shows a history of GPS-UTC obtained from the USNO GPSV1 file. The steering achieved is not as good as clock ensembling can theoretically achieve. Control is not able to reduce the large amplitude ( $\pm 100$  ns) of the offset. It is apparent that the underlying stability of GPS time (without steering) must be considerably worse than 2.3E-14 and/or some other unknown type of aging-like effect, perhaps caused by system model errors, must be going on. Table 1 shows the time steer history from 0000 6 January 1980 to 0630 22 October 1990. Note that steer control values (i.e.,  $\pm 2.00\text{E-}19$  or  $0.00\text{E+}00$ ) only change at times that are multiples of 15 min. (the Kalman filter update interval).

Table 1. Time Steer History

| Day | Month | Year | Modified Julian Date | Time     | Steer Control Value |
|-----|-------|------|----------------------|----------|---------------------|
| 6   | Jan   | 1980 | 44244                | 00:00:00 | +0.00E +00          |
| 25  | Jun   | 1990 | 48067                | 23:30:00 | +2.00E-19           |
| 11  | Jul   | 1990 | 48083                | 22:30:00 | -2.00E-19           |
| 12  | Jul   | 1990 | 48084                | 15:00:00 | +2.00E-19           |
| 13  | Jul   | 1990 | 48085                | 15:00:00 | -2.00E-19           |
| 13  | Jul   | 1990 | 48085                | 21:45:00 | +2.00E-19           |
| 16  | Jul   | 1990 | 48088                | 01:15:00 | -2.00E-19           |
| 16  | Jul   | 1990 | 48088                | 18:30:00 | +2.00E-19           |
| 17  | Jul   | 1990 | 48089                | 05:15:00 | -2.00E-19           |
| 17  | Jul   | 1990 | 48089                | 17:30:00 | +2.00E-19           |
| 19  | Jul   | 1990 | 48091                | 17:00:00 | -2.00E-19           |
| 17  | Aug   | 1990 | 48120                | 16:15:00 | +0.00E +00          |
| 27  | Aug   | 1990 | 48130                | 23:45:00 | -2.00E-19           |
| 28  | Aug   | 1990 | 48131                | 06:30:00 | +2.00E-19           |
| 28  | Aug   | 1990 | 48131                | 17:00:00 | -2.00E-19           |
| 29  | Aug   | 1990 | 48132                | 09:30:00 | +2.00E-19           |
| 29  | Aug   | 1990 | 48132                | 22:15:00 | +0.00E +00          |
| 4   | Sep   | 1990 | 48138                | 16:45:00 | +2.00E-19           |
| 17  | Sep   | 1990 | 48151                | 14:15:00 | +0.00E +00          |
| 21  | Sep   | 1990 | 48155                | 12:15:00 | +2.00E-19           |
| 21  | Sep   | 1990 | 48155                | 12:45:00 | -2.00E-19           |
| 5   | Oct   | 1990 | 48169                | 18:30:00 | +0.00E +00          |
| 9   | Oct   | 1990 | 48173                | 07:15:00 | -2.00E-19           |
| 20  | Oct   | 1990 | 48184                | 11:15:00 | +0.00E +00          |
| 22  | Oct   | 1990 | 48186                | 06:30:00 |                     |

When the steering from Table 1 is backed out of the GPS-UTC plot of Figure 2, along with a mean slope of 4 ns/day, the underlying behavior of GPS-UTC is evident (Figure 3). Ideally Figure 3 should look like random walk with a small amplitude starting from 250 ns offset. The oscillatory nature of this curve needs to be understood. The only source of perturbation on GPS time (or GPS-UTC) must come via the Kalman filter and will occur when the filter is "lied to." For example, if a Rubidium clock (e.g., SV 16) has a large frequency jump and the clock frequency state is not Q'd sufficiently to absorb the variation, then GPS time will be perturbed. It would also be perturbed if an MS suffers a phase or frequency step that goes unnoticed and so the clock covariance is never Q-bumped to allow the filter to solve for the new phase or frequency. GPS time is perturbed because the corrected clock (i.e., the clock time corrected by the filter state offset) represents GPS time, and if the state doesn't correctly compensate for true clock behavior, the "corrected" clock, or GPS time will be perturbed. In the course of these investigations perturbations in both MS and SV clock states were evident, and it is only necessary to see how the filter was handled (e.g., was the covariance matrix Q-bumped or process noise increased at these times) in order to assess whether or not a perturbation in GPS time was likely. An attempt was made to correlate state perturbations occurring in the interval 2 October to 15 October with the slope discontinuities of Figure 3. On 2 October the Multiple Frequency Standard System (i.e., the MFSS of six Cesium clocks operated by the U. S. Naval Research Laboratory (NRL)) at Falcon Air Force Base became the primary standard for the Colorado Springs Monitor Station (COSPM). At the time of the switch, a large jump in the COSPM frequency state was apparent. Hopefully the jump was simultaneous with a large Q-bump of the COSPM clock states, however, the distinct change in slope of GPS-UTC at that time is evidence to the contrary.

#### SV Clock Stability

Although GPS time is being perturbed, due to unmodeled filter processing, the stability of the SV clocks is up to expectations. Figure 4, provided by D. Allan of NIST, is a plot of Allan's variance for five SVs in the constellation. SV 16, the outlier, was having problems during this interval of time (12 August to 11 September 1990). The other four block II SVs are operating better than their specification of 2E-13 at tau equals 1 day. Figures 5 and 6 show SVN 18 clock phase behavior (with a straight line removed) and corresponding Allan variance for tau between 15 min and 1 day. These were computed from MCS Kalman filter data. A 12-hr, unmodeled, periodic variation in phase is evident in Figure 5. Its peak-to-peak amplitude is about 2 m. This periodicity produces the sharp breaks in the Allan variance plot of Figure 6. The 1-day value of the variance, 8E-14, is uncorrupted by the periodicity, since 1 day is a multiple of 12 hr.

#### Stability of GPS Time

It should come as no surprise, because of the oscillatory behavior of GPS-UTC evidenced in Figure 3, that GPS stability relative to UTC (in the interval 31 May to 8 September 1990) would not be as good as predicted from the theory (2.3E-14). This is apparent from Figure 7, another of D. Allan's contributions. Stability is more like 8E-14; comparable to the performance of a master MS configuration.

It should be noted that in the time span of Figure 7, SV 16 had a large frequency jump and in addition its aging state was not being Q'd in the filter. This could have had a significant impact on GPS time. Another impression, however, of GPS time stability is gained when one looks at the Colorado Springs monitor station clock phase state. This state is an estimate of the phase offset between the MFSS ensemble (stable to 2E-14 relative to UTC) and GPS time. The phase state from partition No. 1 is plotted in Figure 8 and its Allan variance is shown in Figure 9. The 1-day GPS stability (with the MFSS stability removed) is 4E-14. The difference between this assessment (based on the current time phase state) and that of D. Allan (based on the predicted phase state) is considerable. The 1-day Allan variance is close to our theoretical expectation. Figure 10, an Allan variance plot for the Kwajalein MS, also supports the idea that GPS time stability is better than 4E-14 at 1 day. The 24-hr periodicity inherent in the clock phase of Kwajalein (and all other MS clocks to a greater or lesser degree) causes the Allan variance to be larger at 12 and 36 hr than at 24 hr. Figure 11 shows this periodicity with peak-to-peak amplitude of 4 m or so. If the clocks are really cycling daily (e.g., because of temperature and/or humidity changes), and the filter estimates only reflect a portion of the amplitude, it is possible that GPS time stability will be degraded for taus that are not a multiple of 24 hr (as Figures 9 and 10 indicate). On the other hand, augmenting the clock model with a sinusoid term would remove the performance degradation. It is also possible that the unmodeled sinusoid is hindering our ability to steer GPS time. This is being investigated by simulation.

As mentioned earlier, each filter partition has its own GPS time reference, and these are reconciled every 15 min for a common value. The effectiveness of this reconciliation is measured by differencing corresponding MS phase states from two partitions. One of these differences for the Kwajalein MS and partitions No.1 and 3 is plotted in Figure 12. Excursions are generally between  $\pm 2$ m. The Allan variance of the difference, a direct measure of the stability of partition No.1 GPS time relative to partition No. 3, is 4E-14 at 1 day (Figure 13). The inferred absolute stability of each relative to a "perfect" clock would be  $4/\sqrt{2}$  E - 14, or 2.7E-14. The stability of GPS time for each partition looks good in terms of Allan variance, but the MS phase difference of  $\pm 2$  m may be a problem. This is being investigated further.

## CONCLUSIONS

GPS time, constructed from the composite clock software, is being perturbed by unmodeled or improperly modeled clock phase behavior. Analysis of Kalman filter MS clock phase estimates shows a daily periodic signature with peak-to-peak amplitude of 4 m that varies somewhat from MS to MS. GPS time stability, inferred from Allan variances of MS clock phase estimates, in the interval 2 to 22 October 1990 very nearly measures up to expectations. This means that the filter clock states are by and large reflecting true clock behavior and, hence, are isolating GPS time from clock perturbations in this interval. Further studies are needed to explain the behavior of GPS-UTC in the interval prior to 2 October when SV 16 was having its problems.

## REFERENCES

1. A. L. Satin and C. T. Leondes "Ensembling Clocks of the Global Positioning System (GPS)," IEEE Transactions on Aerospace and Electronic Systems, Vol. 26, No. 1 (January 1990).
2. K. Brown, "Optimal Ensembling for GPS and Other Systems of Clocks," IBM Federal Systems Division Draft (14 July 1987).
3. A. L. Satin, "Ensembling Clocks of the Global Positioning System," Masters Thesis, Department of Mechanical, Aerospace and Nuclear Engineering, University of California, Los Angeles (1988).
4. Ephemeris/Clock Development Specification, CP-MCSEC-302C, SCN04, Part I, App. A, Navstar GPS Joint Program Office, U.S. Air Force Space Systems Division (1 September 1989).
5. C. H. McKenzie, et al., *GPS-UTC Time Synchronization*, Proceedings of the 21st Annual PTTI Applications and Planning Meeting (28–30 November 1989).

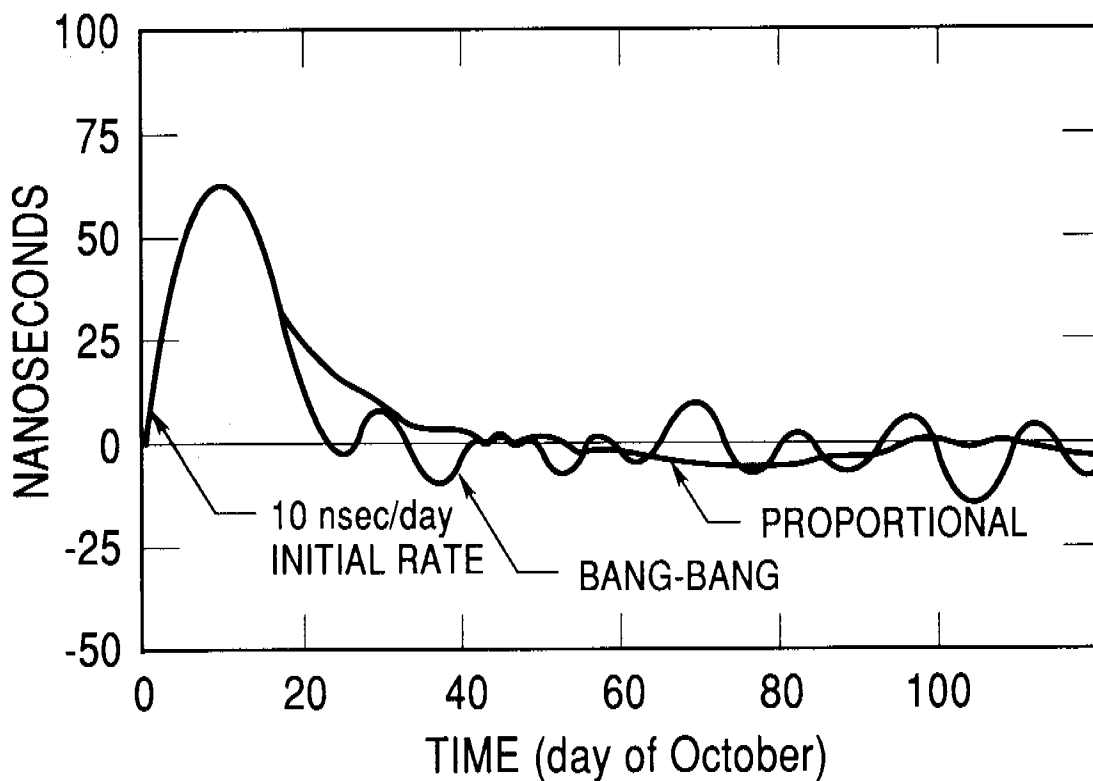


Figure 1. Transient Responses to Bang-Bang and Proportional Steering Control Laws.

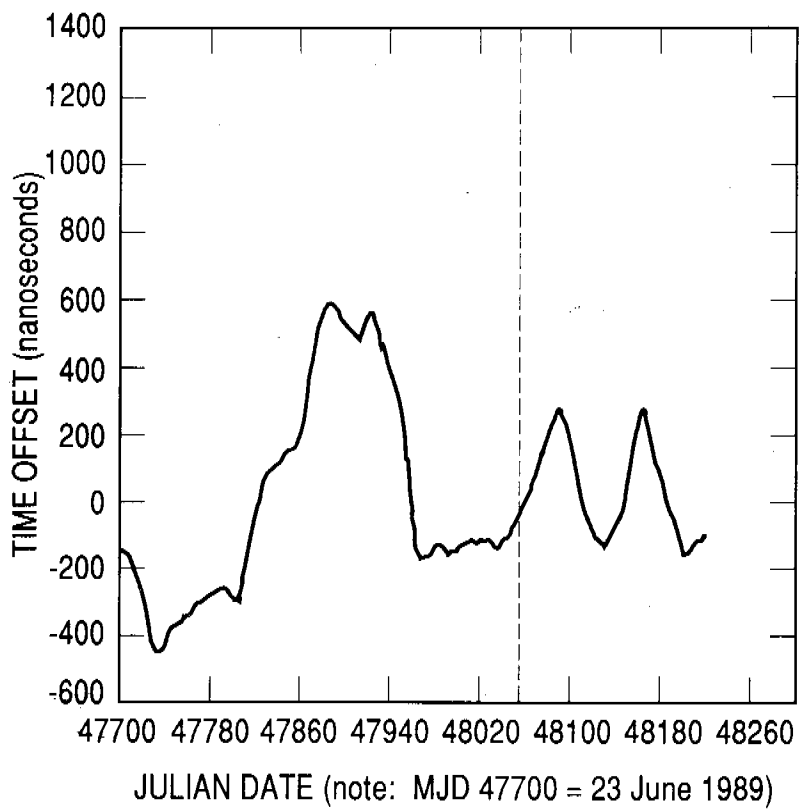


Figure 2. UTC(USNO) Reference — GPS Time

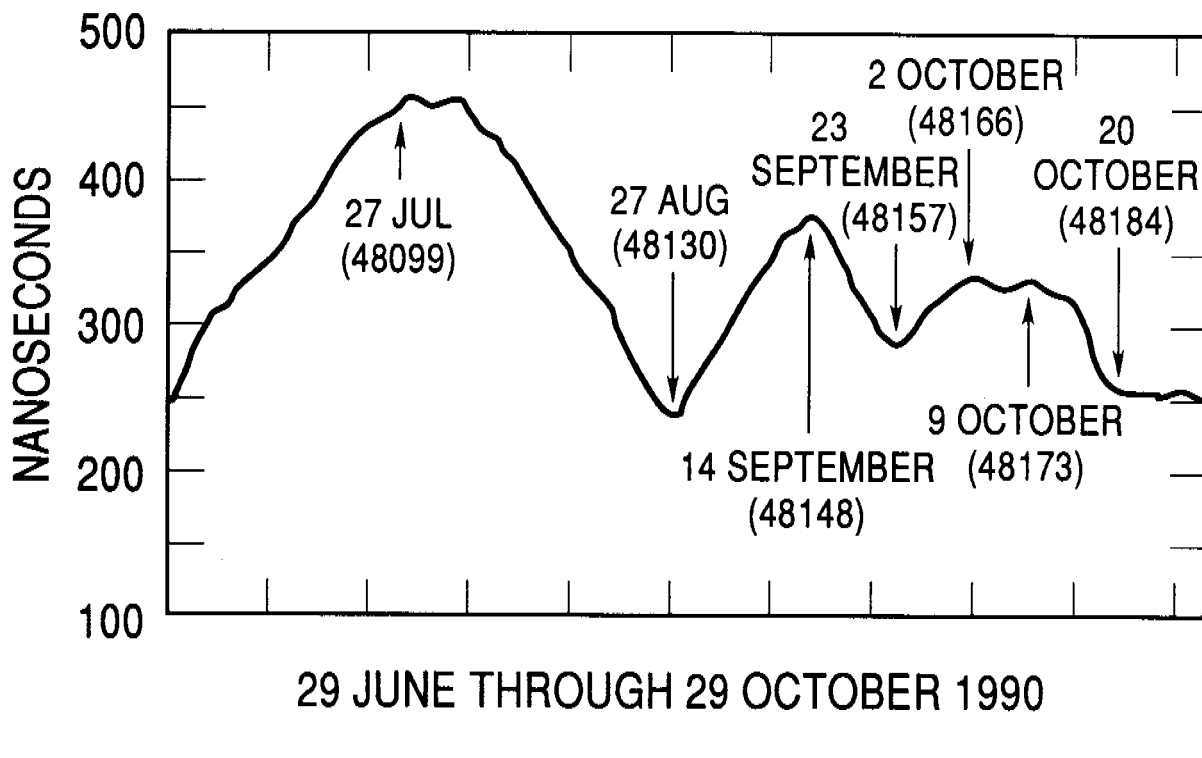


Figure 3. GPS-UTC(USNO) with GPS Time Steering and Mean Slope Removed (4 ns/day).

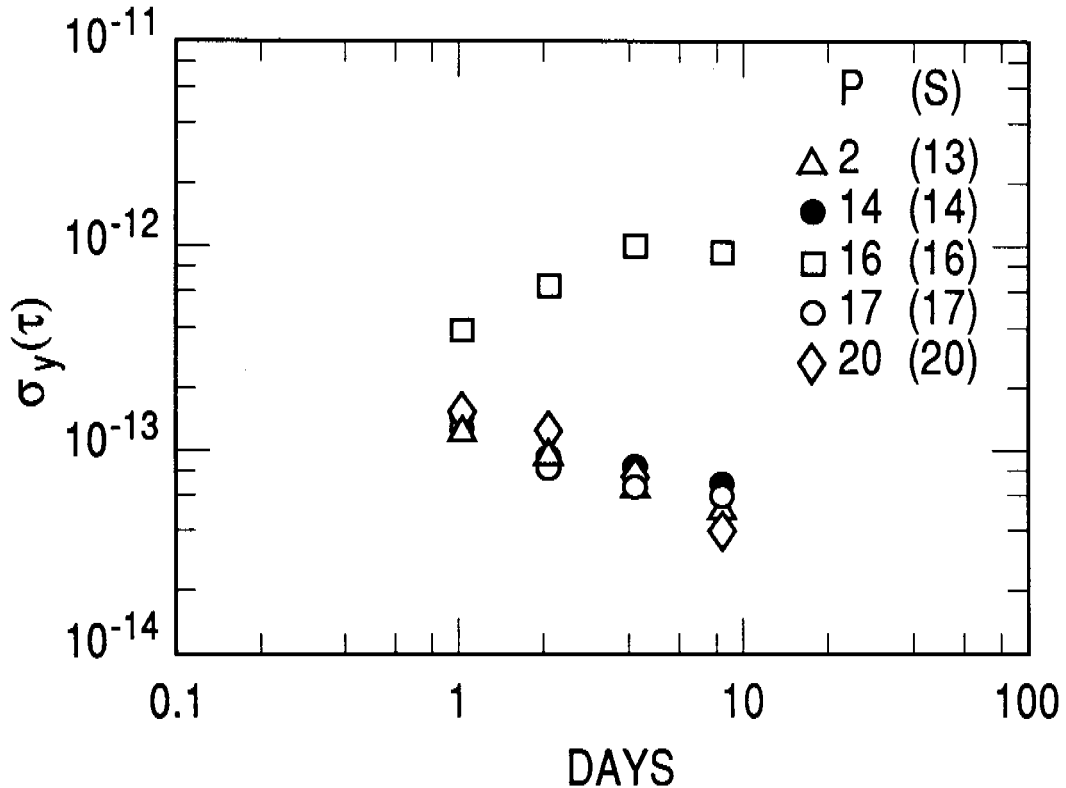


Figure 4. PRN(SVN) Clock — UTC(NIST) 12 August to 11 September 1990.

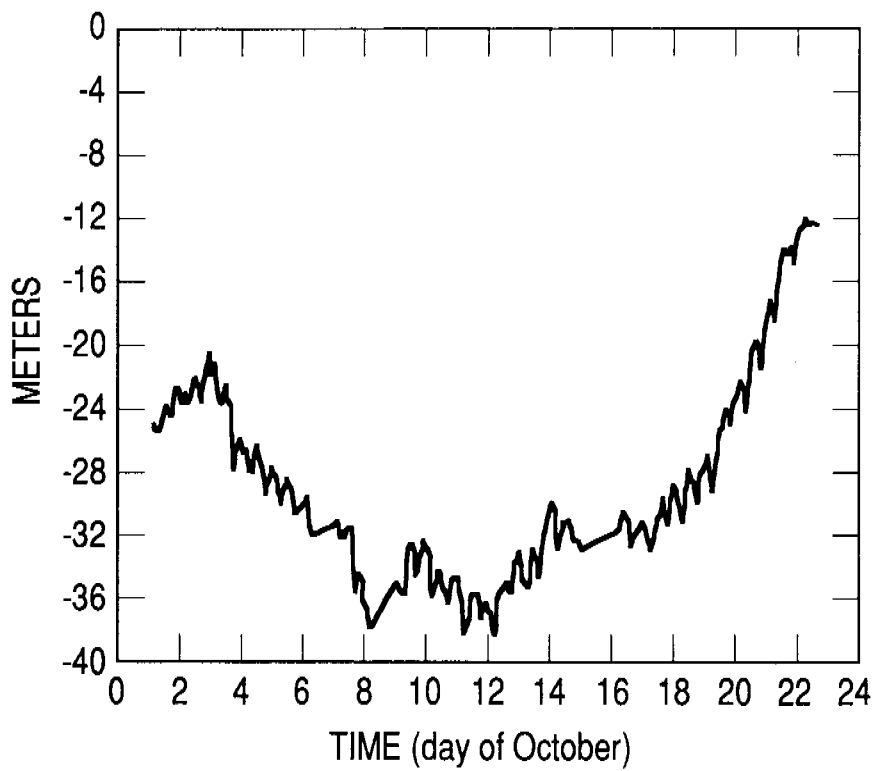


Figure 5. SVN 18 Clock Phase Estimate (2-22 October 1990).

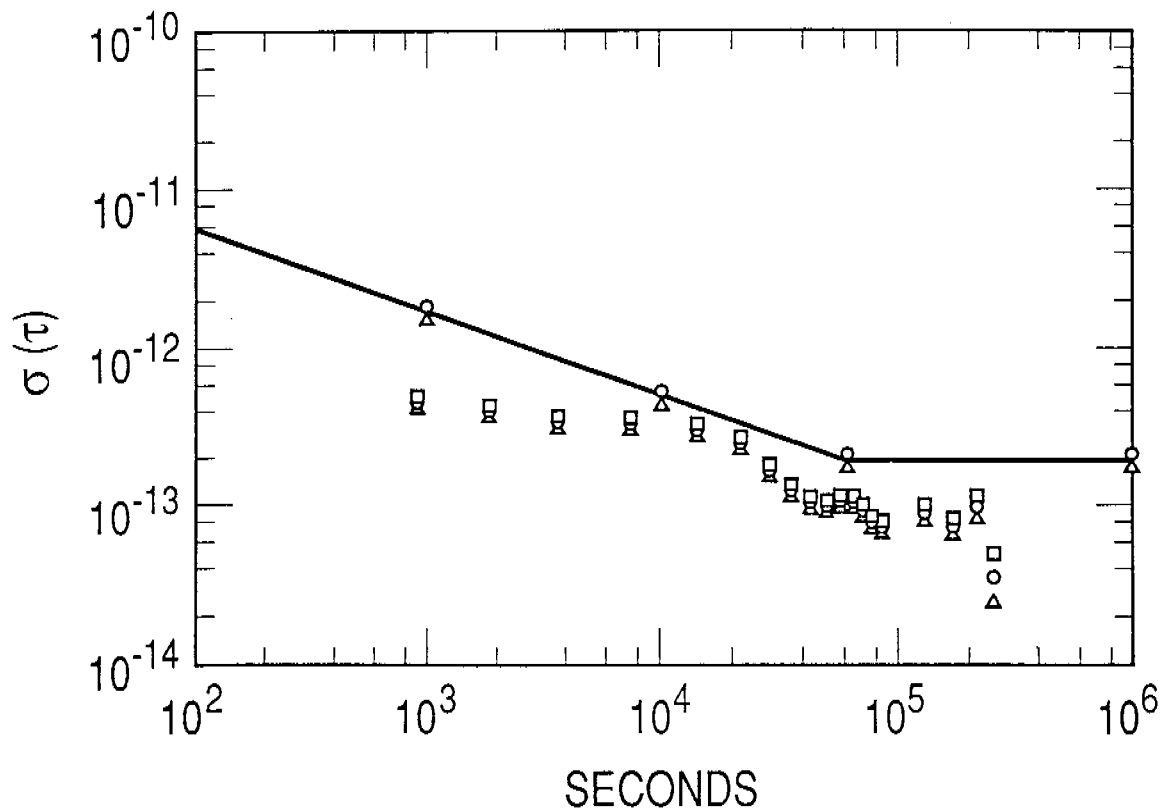


Figure 6. SVN 18 Allan Variance (2-22 October 1990).

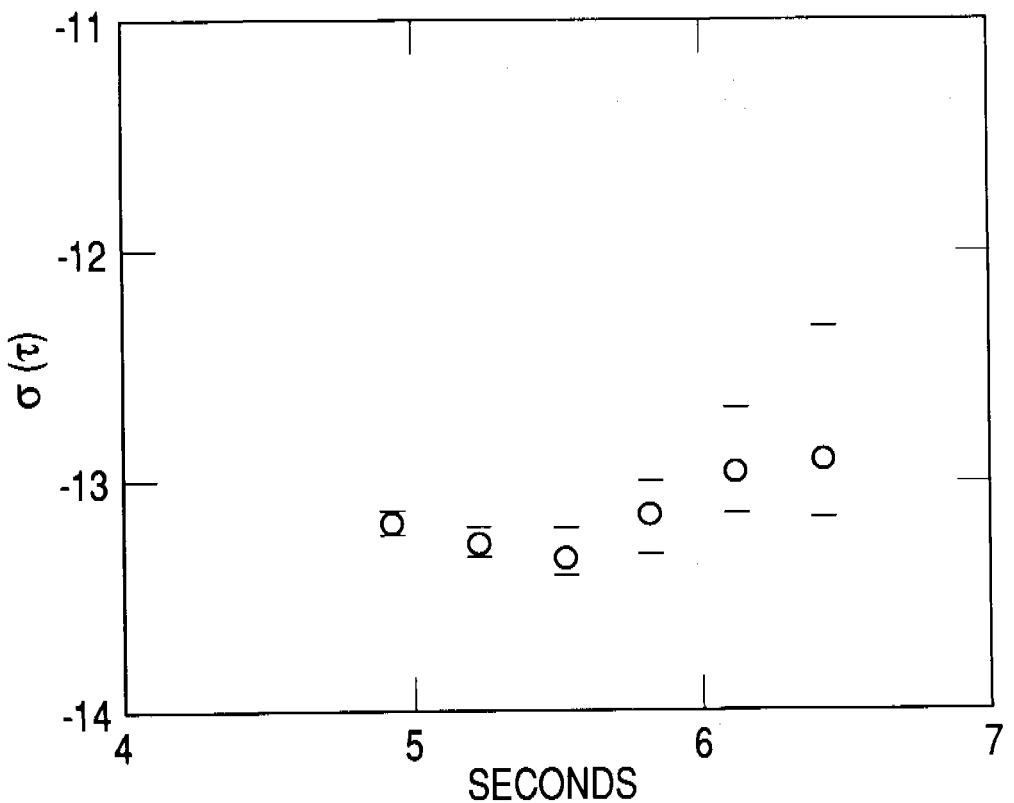


Figure 7. GPS System Time — UTC(USNO MC) (31 May to 8 September 1990).

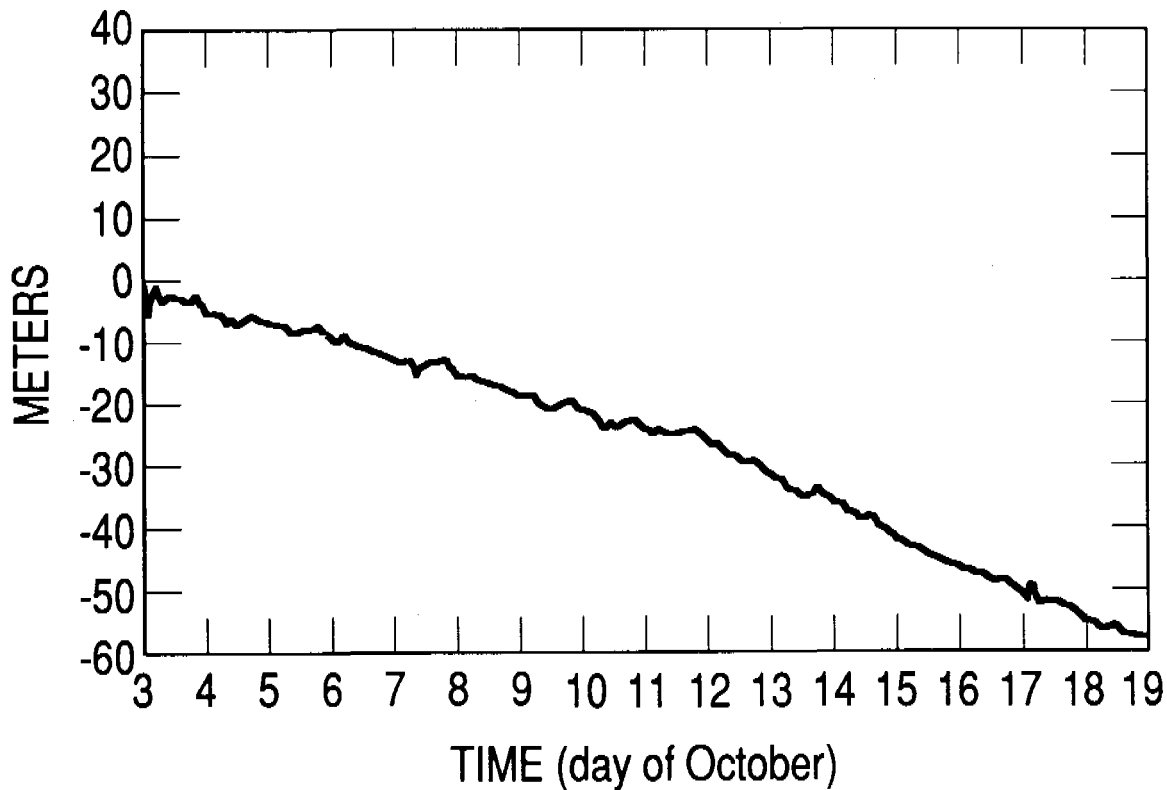


Figure 8. Colorado Springs Monitor Station Clock Phase Estimate (Partition No. 1).

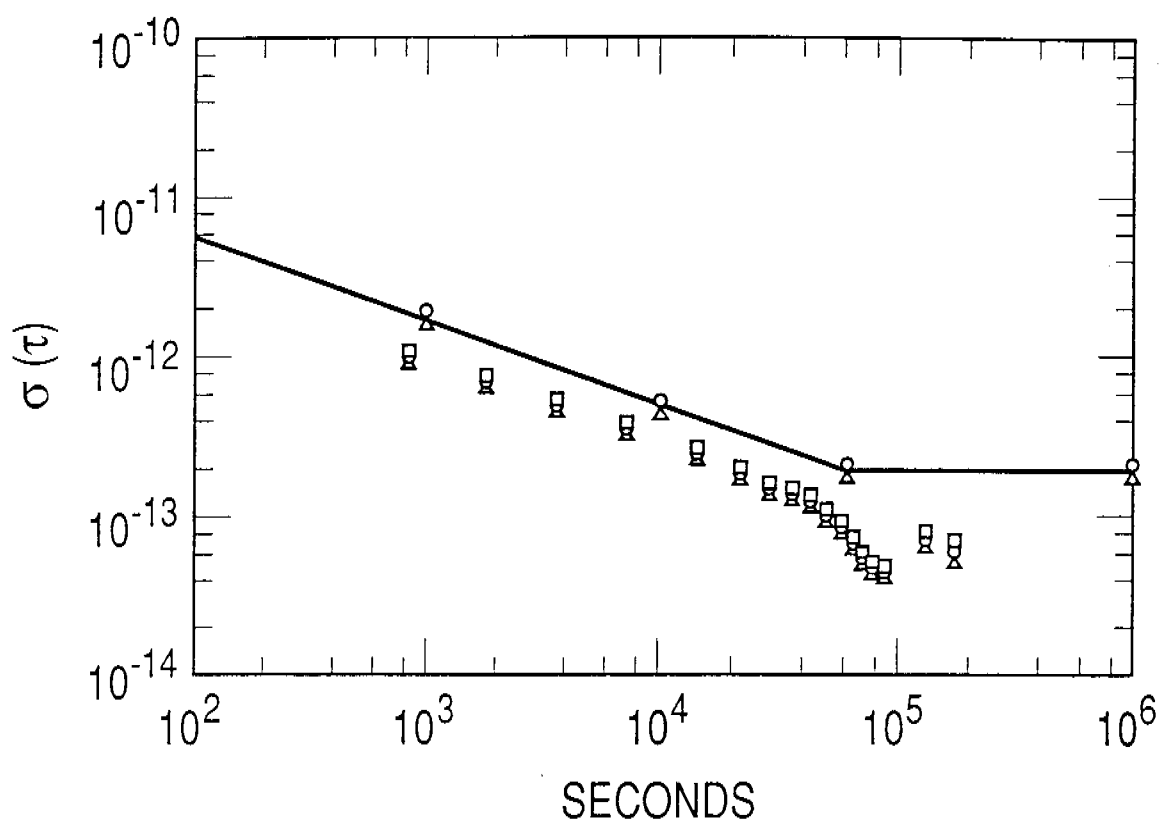


Figure 9. Colorado Springs Monitor Station Allan Variance (Partition No. 1).

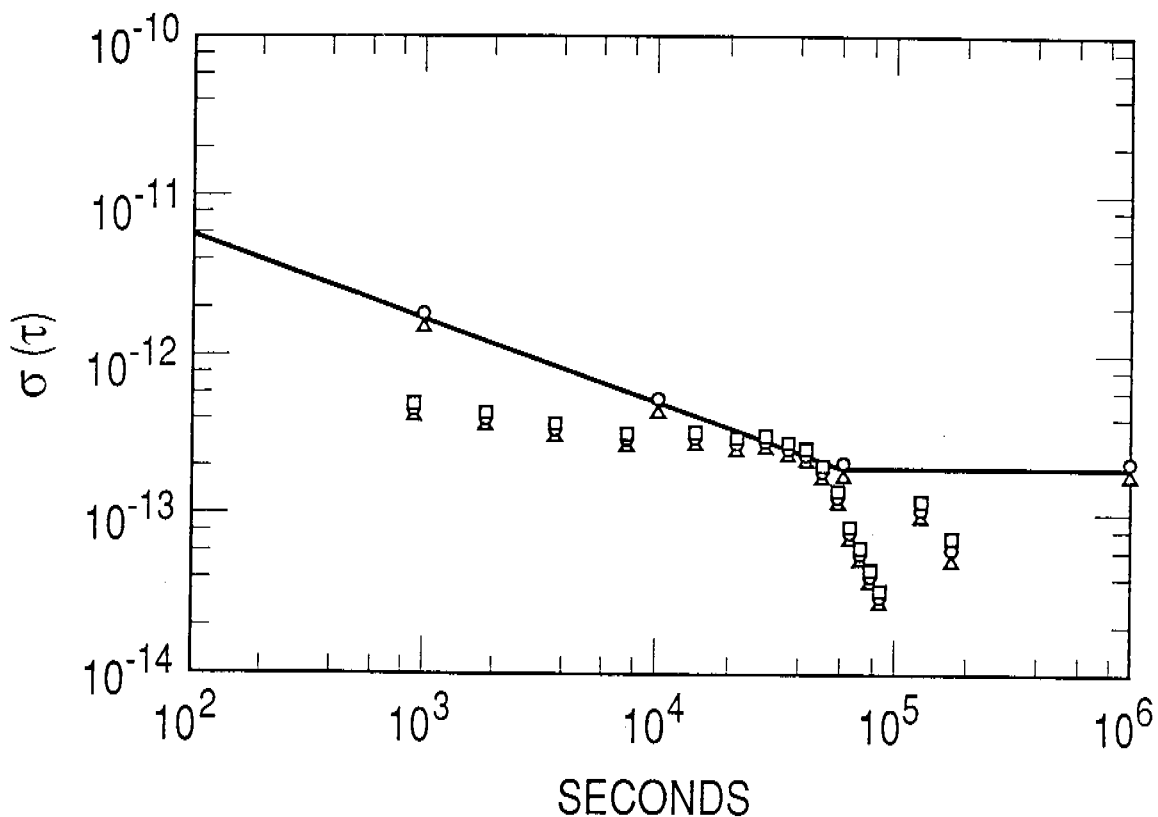


Figure 10. Kwajalein Monitor Station Clock Phase Estimate (3–19 October 1990).

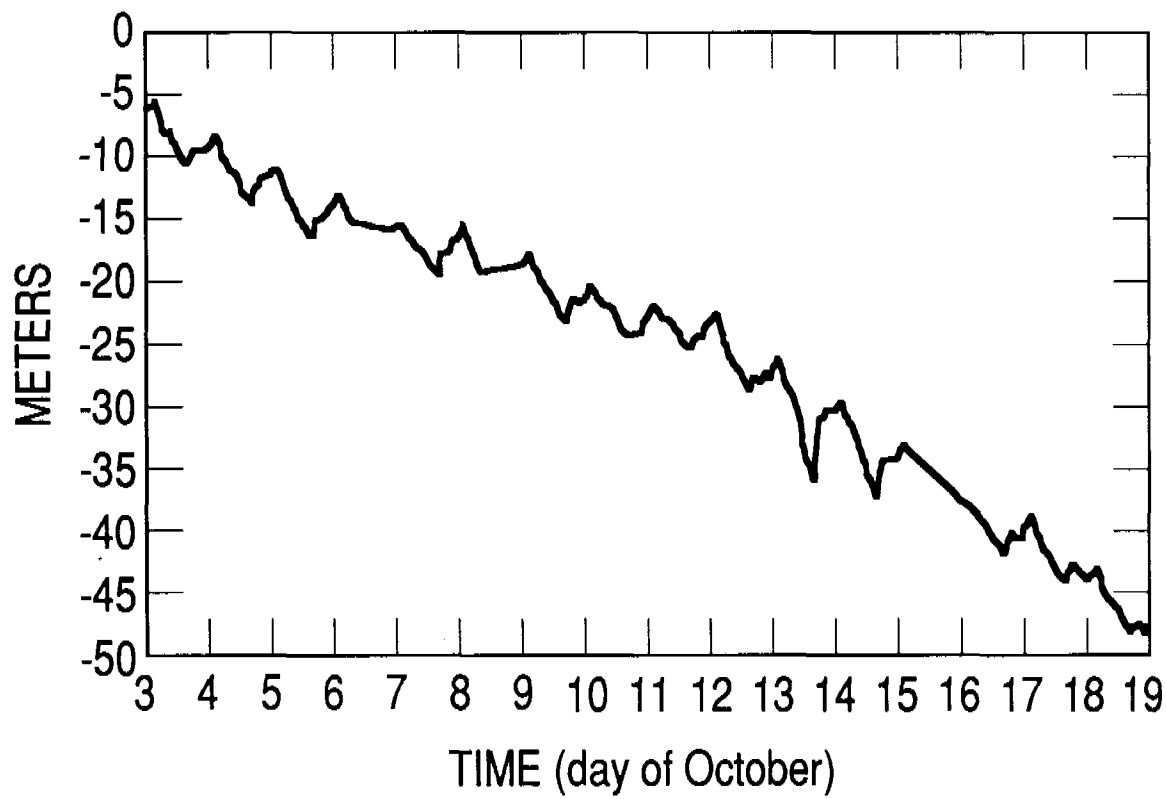


Figure 11. Kwajalein Monitor Station Clock Phase Estimate (3-19 October 1990).

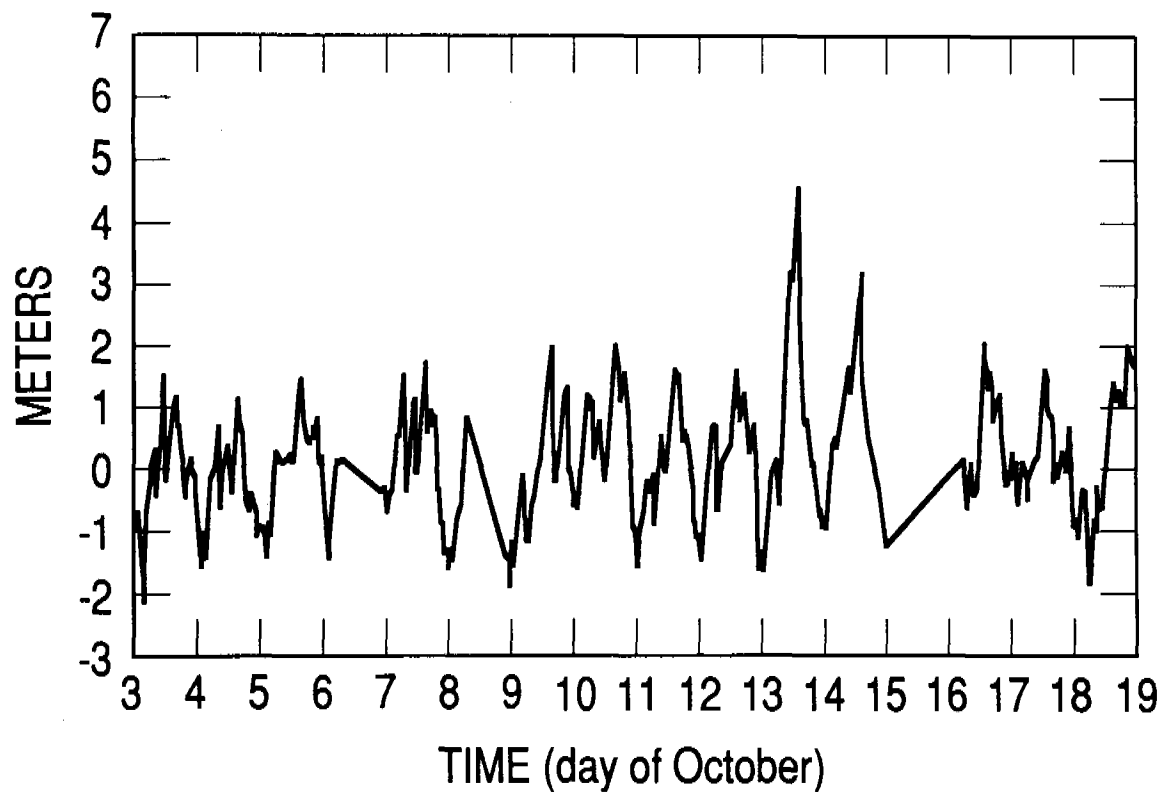


Figure 12. Partition 1 Minus Partition 3 Kwajalein Monitor Station Clock Phase Difference.

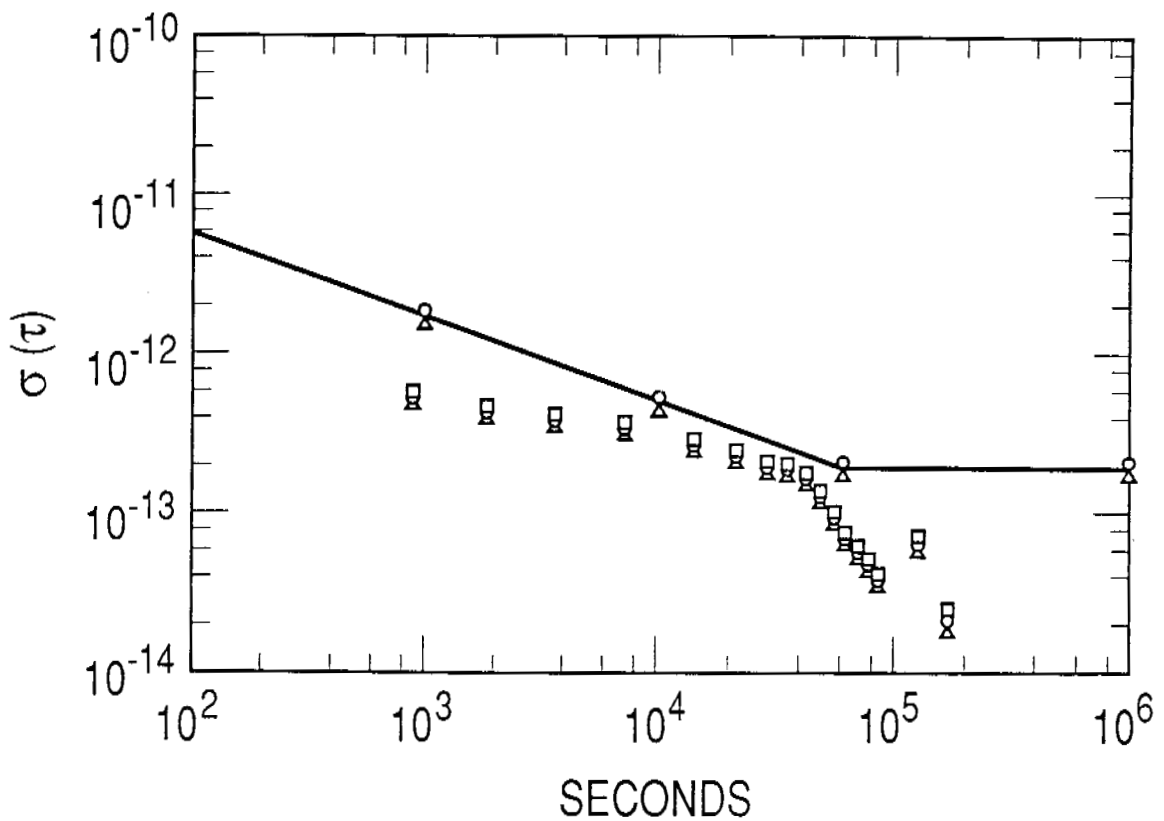


Figure 13. Allan Variance of Partition 1 Minus Partition 3 Kwajalein Monitor Station Clock Phase Difference.

## QUESTIONS AND ANSWERS

**Professor Alley, University of Maryland:** You mentioned that there was a variation. Did that have a 12 hour or a 24 hour period?

**Mr. Satin:** That did not have any definite periodicity to it. It does look like the station frequency has a 24 hour periodicity to it. We think that the periodicity is caused by humidity.

**Professor Alley:** You mentioned a 12 hour period also.

**Mr. Satin:** That is in the satellite, they have a 12 hour orbit. That is a temperature variation effect.

**Dr. Winkler, U. S. Naval Observatory:** What was the rationale which led to the decision to use a bang-bang steering to UTC? And what is the dead-band in that control?

**Mr. Satin:** I can't answer the question about the dead-band right now. We investigated several different algorithms for the control. The bang-bang takes out large initial offsets much quicker than the others.

**Dr. Winkler:** At the expense of much larger frequency changes, and that is, of course, detrimental to its time usage.

**Mr. Satin:** All the simulations show that there is no problem there.

**David Allan, NIST:** On your last view-graph, the cesium performance of  $\tau^{-1/2}$  from  $10^{-12}$  down to  $10^{-13}$  is pretty typical of the space cesiums. How can you have a  $\tau^{-1}$  type of behavior out at  $10^5$  seconds? That is not typical of cesiums or anything in the system.

**Mr. Satin:** We think that that is related to the periodicity in the monitor stations. In other words, at the 24 hour point you don't see the 24 periodicity and things get better, but you do see it at other points.

**Mr. Allan:** You are saying that this is an aliasing?

**Mr. Satin:** Yes, that is right.

**Mr. Allan:** But if you have a periodicity, it will increase the noise over  $\tau^{-1/2}$ , it will not decrease it. The curve would have an increase at 12 hours, and no increase at 24 hours. You have a  $\tau^{-1/2}$  curve, so I don't see any aliasing affect.

**Dr. Henry Fliegel, The Aerospace Corporation:** We believe that the strange appearance of the sigma-tau curve is because we do have 24 hour periodicities and they alias at 12 and 36 hours. As far as I know, that completely explains the appearance of the curve.

**Dr. Claudine Thomas, BIPM:** Why are you using that set of filters and the clocks are not

independent, when with one Kalman filter you could handle everything?

**Mr. Satin:** It is computationally more efficient to use three smaller filters. When the system was first designed, we didn't have the number-crunching capability to handle the single Kalman filter. That would be 24 satellites, 11 states per satellite for a total of hundreds of states.

**Dr. Thomas:** Yes, but the clocks which are involved in your filters are not independent.

**Mr. Satin:** Right, it is sub-optimal. That is correct, but we did a study to determine what the effect would be to use one, two, or three filters because we are making a large software change and could change the filters, but the gain was essentially zero.

**Sam Stein, Ball Corp.:** I am afraid, Henry, that I would have to agree with Dave Allan and disagree with you. We calculated the exact effect of a periodicity on  $\sigma_y$ . Its effect, if you have a 24 hour periodicity, would be an elevation of  $\sigma_y$  over the white frequency noise level, due to the ensemble, at 12 hours, a decrease back to the white frequency noise level at 24 hours, and then it would come back up afterwards. If you look at the very short term, if you look at the numbers at 1000 seconds, you can see where the  $\tau^{-1/2}$  level is. Whatever this phenomenon is, it causes a decrease below the noise level that one would attribute to the ensemble, and that is surprising. We often see this when there is a small amount of data, but if those are error bars that I see on the curve, it would indicate that there is an adequate amount of data and one should not see such a large effect.

**Mr. Satin:** We have approximately 20 days of data, so we should have a pretty good estimate of the one day variance.

**Tom McCaskill, Naval Research Laboratory:** I would just like to make some comments. If you look at the short term data, you start out at 900 seconds, which is 15 minutes. If you follow that out, you have the same slope out to what corresponds to the time for one pass of a satellite. Then there is the time when you are switching to another satellite and you get a different type of behavior. I agree with the other gentlemen about the effect of the periodicity, but this is not that effect.